Spin entanglement induced by spin-orbit interactions in coupled quantum dots

Nan Zhao,[1] L. Zhong,[2] Jia-Lin Zhu,[1] and C. P. Sun[2]
[1]*Department of Physics, Tsinghua University, Beijing 100084, China*
[2]*Institute of Theoretical Physics, Chinese Academy of Sciences, Beijing, 100080, China*
(Received 5 April 2006; published 3 August 2006)

We theoretically explore the possibility of creating spin quantum entanglement in a system of two electrons confined respectively in two vertically coupled quantum dots in the presence of Rashba-type spin-orbit coupling. We find that the system can be described by a generalized Jaynes-Cummings model of two-mode bosons interacting with two spins. The lower excited states of this model are calculated to reveal the underlying physics of the far-infrared absorption spectra. The analytic perturbation approach shows that an effective transverse coupling of spins can be obtained by eliminating the orbital degrees of freedom in the large-detuning limit. Here, the orbital degrees of freedom of the two electrons, which are described by two-mode bosons, serve as a quantized data bus to exchange the quantum information between the two electron spins. Then a nontrivial two-qubit logic gate is realized and spin entanglement between the two electrons is created by virtue of spin-orbit interactions.

DOI: 10.1103/PhysRevB.74.075307 PACS number(s): 68.65.Hb, 71.70.Ej, 03.65.−w, 03.67.Mn

I. INTRODUCTION

Control and manipulation of the spin degrees of freedom has become one of the most important topics both in spintronics[1] and in quantum information processing.[2] The spin-orbit interaction (SOI) in semiconductor heterostructures provides a way to couple electron spins with their orbital degrees of freedom, and consequently has attracted more and more attention in recent years. The spin properties of a few electrons confined in semiconductor nanostructures, such as quantum dots,[3–8] coupled quantum dots,[9] quantum rings,[10] and quantum wires,[11] have been studied. The results show that the carrier's spin properties are strongly affected in the presence of the SOI, and novel features emerge in these nanostructures compared with the traditional ones without the SOI.

On the other hand, the spin confined in a quantum dot is a natural choice for the physical realization of a qubit. This kind of system is considered as an important candidate for solid-state-based quantum computing. Among various approaches to implementing quantum information processing using quantum dot systems, optical methods, using the classical laser field[12] and quantized cavity modes,[13] have been proposed to create entanglement and to realize single- and double-qubit logic gates. In Ref. 15, a scheme with quantum dots embedded in an optical cavity was designed, so that the cavity mode can serve as a data bus and induce a spin-spin interaction. This kind of cavity-mediated two-qubit gates are studied in detail for several other solid-state systems very recently.[16]

Now we note that the SOI phenomena in nanostructures have been investigated with the help of quantum optics methods. Taking advantage of the tunability of the SOI strength, an experiment to observe coherent oscillations in a single quantum dot was proposed in Ref. 3. In this proposal, the orbital degrees of freedom are modeled by two boson modes. Under the rotating-wave approximation (RWA), the SOI of an electron confined in a single quantum dot was reduced to a Jaynes-Cummings (JC) model, which is a very typical model in quantum optics. This analogy between the SOI in a quantum dot and the JC model in cavity QED suggests that it is possible to make use of the orbital degrees of freedom, instead of the real optical cavity modes, to serve as a quantized data bus, and then to induce a spin entanglement.[14]

In this paper, we propose and study a model of two electrons confined in two vertically coupled quantum dots (CQDs) respectively with Rashba-type SOI, and explore the possibility of realizing a nontrivial two-qubit logic gate or creating spin entanglement in this system. For simplicity, we consider two vertically coupled quantum dots with two-dimensional parabolic confinement. In the case of strong confinement and large interdot separation, the Coulomb interaction between the two electrons is approximately expanded to second order, and then the orbit motions of the two-electron system can be reduced to four-mode bosons. Under the RWA, only two of the four modes are coupled with the spin degrees of freedom. Then it is proved that the total system with SOI can be effectively described by a generalized JC model with coupling between two-mode bosons and two spins. By diagonalizing the Hamiltonian directly in the lower excited subspace, the eigenvalues and the corresponding eigenfunctions are obtained exactly. The far infrared (FIR) absorption spectra are calculated according to these analytical solutions, which help us to understand the underlying physics of the spectra. To get the effective Hamiltonian of spin-spin interaction, we perform the Fröhlich transformation in the large-detuning limit. This effective Hamiltonian can dynamically drive a two-qubit logic gate operation. By using the conventional material parameters, our numerical estimation shows that the effective spin interaction induced by SOI is quite strong, compared to the spin decoherence in low-dimensional semiconductor structures. It is feasible experimentally to implement a two-qubit logic gate, and thus to produce quantum entanglement.

The paper is organized as follows. In Sec. II, the generalized JC model is derived from the original Hamiltonian of two electrons confined in two quantum dots. Analytical solutions of lower excited states and FIR spectra are presented

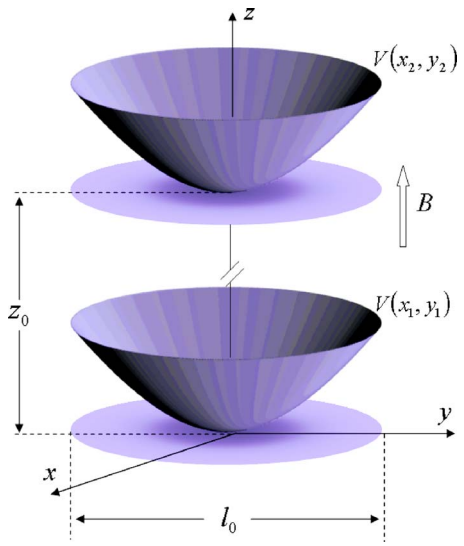

FIG. 1. (Color online) Schematic illustration of vertically stacked quantum dots. Each quantum dot confines an electron. We assume that the interdot separation z_0 is larger than the characteristic length of quantum dot confinement, l_0.

in Sec. III. In Sec. IV, we show that the perturbation treatment gives the effective transverse spin-spin interaction in the large-detuning limit, and demonstrate that a two-qubit logic gate and quantum entanglement can be achieved in this kind of system with SOI.

II. TWO-MODE JC MODEL FOR VERTICALLY CQDS WITH SOI

We consider two vertically CQDs with an interdot separation z_0 (see Fig. 1). Each quantum dot is described by a two-dimensional parabolic confinement potential $V(r_i)=m_0\omega_0^2 r_i^2/2$ with the basic frequency ω_0. Including the Rashba-type SOI

$$H_{\mathrm{SO}}^{(i)}=\frac{\alpha}{\hbar}[\sigma_i\times\mathbf{\Pi}_i]_z, \tag{1}$$

the Zeeman term

$$H_Z^{(i)}=\frac{1}{2}g\mu_B\mathbf{B}\cdot\sigma_i, \tag{2}$$

and the Coulomb interaction

$$V_{\mathrm{Coul}}(|\mathbf{r}_1-\mathbf{r}_2|)=\frac{e^2}{4\pi\varepsilon\varepsilon_0|\mathbf{r}_1-\mathbf{r}_2|}, \tag{3}$$

the total Hamiltonian reads

$$H=\sum_{i=1,2}\left(\frac{\mathbf{\Pi}_i^2}{2m_0}+V(r_i)+H_{\mathrm{SO}}^{(i)}+H_Z^{(i)}\right)+V_{\mathrm{Coul}}. \tag{4}$$

Here, $-e$, μ_B, and ε_0 are the electron charge, Bohr magneton, and dielectric constant in vacuum, respectively. m_0, g, and ε are the material-related parameters of effective mass, Landé g factor, and relative dielectric constant, respectively. $\mathbf{\Pi}_i=\mathbf{p}_i+e\mathbf{A}(\mathbf{r}_i)$ is the canonical momentum and $\mathbf{A}(\mathbf{r}_i)=B(-y_i/2,x_i/2,0)$ is the vector potential for magnetic field $\mathbf{B}=B\hat{\mathbf{z}}$.

In order to simplify the Coulomb interaction, we consider a special case in which the interdot separation z_0 is much larger than the lateral confinement characteristic length $l_0=\sqrt{\hbar/m_0\omega_0}$, i.e., $(l_0/z_0)^2\ll 1$. Then we expand the Coulomb interaction as a power series of the relative coordinate $r=|\mathbf{r}_1-\mathbf{r}_2|$ up to the second order:[17,18]

$$V_{\mathrm{Coul}}(r)\simeq V_0-\frac{1}{2}m_0\omega_1^2 r^2. \tag{5}$$

Here, we have defined $V_0=e^2/(4\pi\varepsilon\varepsilon_0 z_0)$, and $\hbar\omega_1=\sqrt{\hbar^2 V_0/m_0 z_0^2}$. We also assume that the two electrons are strictly confined to the two quantum dots, respectively, and then neglect the overlap of their wave functions.

In the center of mass (c.m.) reference frame defined by $\mathbf{R}=(\mathbf{r}_1+\mathbf{r}_2)/2$ and $\mathbf{r}=\mathbf{r}_1-\mathbf{r}_2$, we have the c.m. and relative momenta $\mathbf{P}=\mathbf{p}_1+\mathbf{p}_2,\mathbf{p}=(\mathbf{p}_1-\mathbf{p}_2)/2$, and the corresponding angular momenta $\mathbf{L}=\mathbf{R}\times\mathbf{P}$, $\boldsymbol{l}=\mathbf{r}\times\mathbf{p}$, where $M=2m_0$, $m=m_0/2$, $\mathbf{r}$ is the relative coordinate, and $\mathbf{R}$ is the c.m. coordinate. The orbital part of the Hamiltonian is expressed in a quadrature form of these coordinates:

$$H_{orbit}=\sum_{i=1,2}\left(\frac{\mathbf{\Pi}_i^2}{2m_0}+V(r_i)\right)+V_{\mathrm{Coul}}$$

$$=\frac{P^2}{2M}+\frac{1}{2}M\Omega^2R^2+\frac{1}{2}\omega_c L_z+\frac{p^2}{2m}+\frac{1}{2}m\omega^2r^2+\frac{1}{2}\omega_c l_z. \tag{6}$$

Here, the cyclotron frequency is $\omega_c=eB/m_0$, and the frequencies of c.m. and relative motion are $\Omega=\sqrt{\omega_0^2+\omega_c^2/4}$ and $\omega=\sqrt{\Omega^2-2\omega_1^2}$, respectively. Note that the effect of the Coulomb repulsion is to reduce the relative motion to a lower frequency compared to the c.m. motion. In our model the requirement $(l_0/z_0)^2\ll 1$ ensures that $\omega>0$ is satisfied even when $B=0$.

We define the boson operators $a_x,a_x^\dagger,a_X$, and $a_X^\dagger$ of the x components by

$$X=\sqrt{\frac{\hbar}{2M\Omega}}(a_X^\dagger+a_X),$$

$$x=\sqrt{\frac{\hbar}{2m\omega}}(a_x^\dagger+a_x),$$

$$P_X=i\sqrt{\frac{\hbar M\Omega}{2}}(a_X^\dagger-a_X),$$

$$p_x=i\sqrt{\frac{\hbar m\omega}{2}}(a_x^\dagger-a_x); \tag{7}$$

and the boson operators $a_y,a_y^\dagger,a_Y$, and $a_Y^\dagger$ of the y components are defined in a similar way. Let

$$A=(a_X+ia_Y)/\sqrt{2},$$

$$a=(a_x+ia_y)/\sqrt{2},$$

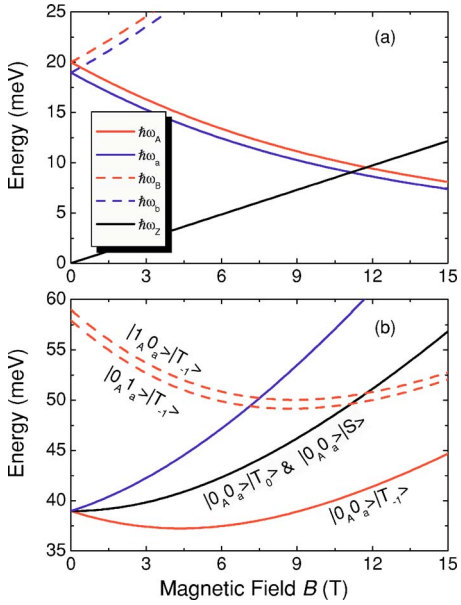

FIG. 2. (Color online) (a) Energy dispersions with respect to the magnetic field B of the four modes of the boson frequencies ω_A [red (light gray) solid line], ω_a [blue (dark gray) solid line], ω_B [red (light gray) dashed line], and ω_b [blue (dark gray) dashed line], and the Zeeman energy ω_z (black line). (b) Energy spectrum of H_0. Different lines correspond to different spin and orbit states, which are indicated explicitly in the figure. The parameters used in calculation are listed in Table I.

$$B = (a_X - ia_Y)/\sqrt{2},$$

$$b = (a_x - ia_y)/\sqrt{2}. \tag{8}$$

Then we rewrite the orbit Hamiltonian (6) in terms of four-mode bosons A, a, B, and b as

$$H_{\text{orbit}} = \hbar\,\omega_A(A^\dagger A + 1/2) + \hbar\,\omega_B(B^\dagger B + 1/2) + \hbar\,\omega_a(a^\dagger a + 1/2) + \hbar\,\omega_b(b^\dagger b + 1/2), \tag{9}$$

with their frequencies, respectively,

$$\omega_A = \Omega - \frac{1}{2}\omega_c, \quad \omega_B = \Omega + \frac{1}{2}\omega_c, \tag{10}$$

$$\omega_a = \omega - \frac{1}{2}\omega_c, \quad \omega_b = \omega + \frac{1}{2}\omega_c. \tag{11}$$

These four frequencies, together with the Zeeman energy $\hbar\omega_z = |g|\mu_B B$ are drawn in Fig. 2(a) with respect to the magnetic field B. Note that the Zeeman energy $\hbar\omega_z$ and the boson frequencies ω_A and ω_a reach the resonant region at $B \simeq 11$ T with the parameters listed in Table I. We also draw the lower-energy spectra of the orbit Hamiltonian (6) in Fig. 2(b). We will focus on how these states are affected in the presence of SOI in the following sections.

In terms of the four-mode boson operators defined by Eqs. (7) and (8), the SOI Hamiltonian H_{SO}, after some straightforward algebra, can be rewritten as

TABLE I. Parameters [for InAs (Ref. 6)] used in the calculations.

Quantity	Value
m_0	0.042
ε	14.6
g	−14
α	10 meV nm
ω_0	20 meV
l_0	9.5 nm
z_0	20 nm

$$H_{\text{SO}}^{\text{RWA}} = g_A A(\sigma_{1+} + \sigma_{2+}) + g_a a(\sigma_{1+} - \sigma_{2+}) + \text{H.c.} \tag{12}$$

Note that, due to the negative value of the Landé g factor, a unitary rotation $\sigma_z \mapsto -\sigma_z$ and $\sigma_\pm \mapsto -\sigma_\mp$ has been performed.[3] To obtain the interaction Hamiltonian above, we have used the RWA to neglect the counter-rotating terms like $\sigma_+ B^\dagger, \sigma_+ b^\dagger, \sigma_- B$, and $\sigma_- b$. This approximation has been verified numerically for the single-electron case in Ref. 3. The coupling strengths g_A and g_a are defined as follows:

$$g_A = \alpha\sqrt{\frac{m_0\Omega}{2\hbar}}\left(1 - \frac{\omega_c}{2\Omega}\right), \tag{13}$$

$$g_a = \alpha\sqrt{\frac{m_0\omega}{2\hbar}}\left(1 - \frac{\omega_c}{2\omega}\right). \tag{14}$$

So far, we have obtained a generalized JC model where two-mode bosons interact with two spins. In the following sections we will further demonstrate how the orbit motion induces a spin-spin entanglement in the presence of SOI.

III. LOWER EXCITED STATES AND FIR SPECTRA

In this section, we calculate the eigenenergies and eigenstates of the low excited states. Notice that the total excitation number operator

$$\hat{N} = a^\dagger a + A^\dagger A + \frac{1}{2}(\sigma_{1z} + \sigma_{2z}) \tag{15}$$

commutes with $H = H_{\text{orbit}} + H_Z^{(1)} + H_Z^{(2)} + H_{\text{SO}}^{\text{RWA}}$. For a given integer N, which is the eigenvalue of $\hat{N}$, the dimension of the invariant subspace $V^{(N)}$ is $4N+4$ for $N \geq 0$.

The lowest subspace $V^{(-1)}$, corresponding to $N=-1$, is of one dimension. The ground state can be directly written as $|\text{GS}\rangle = |0_A, 0_a, 0_B, 0_b, \downarrow, \downarrow\rangle$, which means the excitation numbers of boson modes n_A, n_a, n_B and n_b are zero, i.e.,

$$n_A = n_a = n_B = n_b = 0, \tag{16}$$

and both spins are in the down state. The corresponding eigenenergy is

$$E_{\text{GS}} = \frac{\hbar}{2}(\omega_A + \omega_B + \omega_a + \omega_b - 2\omega_z). \tag{17}$$

The second lowest subspace $V^{(0)}$ is of four dimensions. The Hamiltonian can be exactly diagnolized in this subspace. We define

$$|S\rangle = \frac{1}{\sqrt{2}}(|0_A,0_a,\uparrow,\downarrow\rangle - |0_A,0_a,\downarrow,\uparrow\rangle),$$

$$|T_0\rangle = \frac{1}{\sqrt{2}}(|0_A,0_a,\uparrow,\downarrow\rangle + |0_A,0_a,\downarrow,\uparrow\rangle),$$

$$|T^A_{-1}\rangle = |1_A,0_a,\downarrow,\downarrow\rangle, |T^a_{-1}\rangle = |0_A,1_a,\downarrow,\downarrow\rangle, \tag{18}$$

where both n_B and n_b are zero, and they are omitted in the state notations for simplicity. The eigenstates of the Hamiltonian in this subspace are

$$|\Phi^+_A\rangle = \sin\frac{\theta_A}{2}|T^A_{-1}\rangle + \cos\frac{\theta_A}{2}|T_0\rangle, \tag{19}$$

$$|\Phi^-_A\rangle = \cos\frac{\theta_A}{2}|T^A_{-1}\rangle - \sin\frac{\theta_A}{2}|T_0\rangle, \tag{20}$$

$$|\Phi^+_a\rangle = \sin\frac{\theta_a}{2}|T^a_{-1}\rangle + \cos\frac{\theta_a}{2}|S\rangle, \tag{21}$$

$$|\Phi^-_a\rangle = \cos\frac{\theta_a}{2}|T^a_{-1}\rangle - \sin\frac{\theta_a}{2}|S\rangle, \tag{22}$$

and the corresponding eigenvalues are

$$E^\pm_A = -\frac{\Delta_A}{2} \pm \sqrt{\left(\frac{\Delta_A}{2}\right)^2 + 2g_A^2}, \tag{23}$$

$$E^\pm_a = -\frac{\Delta_a}{2} \pm \sqrt{\left(\frac{\Delta_a}{2}\right)^2 + 2g_a^2}. \tag{24}$$

Here, the zero-point energies of the four boson modes are omitted. $\theta_{A,a}$ are defined as

$$\tan\theta_{A,a} = \frac{2\sqrt{2}g_{A,a}}{\Delta_{A,a}} \tag{25}$$

where $\theta_{A,a} \in [0,\pi]$, and $\Delta_{A,a} = \omega_z - \omega_{A,a}$.

With the help of these exact eigenenergies and eigenstates obtained above, we can calculate the FIR absorption spectra analytically. To this end, we consider the time-dependent Hamiltonian of the system in an optical field,

$$\tilde{H}(t) = H + H'e^{-i\omega t} + \text{H.c.} \tag{26}$$

where $H'e^{-i\omega t}$ is the time-dependent term induced by the classical optical field[6]

$$H' \propto -\sum_{i=1,2}\left(\frac{ea}{m}\boldsymbol{\epsilon}\cdot(\mathbf{p}_i + e\mathbf{A}_i) + \frac{\alpha ea}{\hbar}(\sigma_i \times \boldsymbol{\epsilon})_z\right), \tag{27}$$

where a is the radiation field amplitude, and $\boldsymbol{\epsilon} = (\hat{x} - i\hat{y})/\sqrt{2}$ is the polarization vector for circularly polarized light.

The absorption coefficient is calculated according to the Fermi golden rule[19,20]

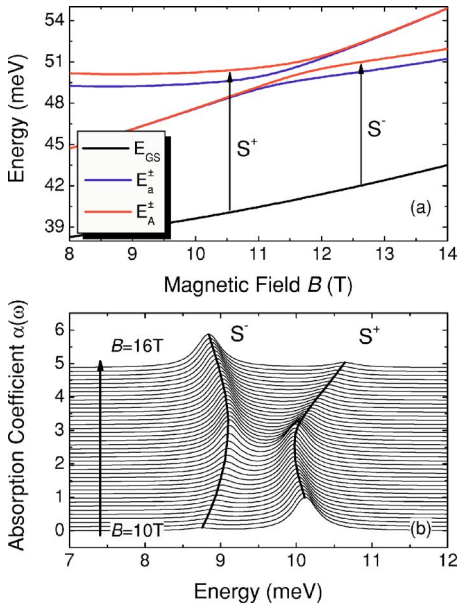

FIG. 3. (Color online) (a) Exact energy spectra given by Eqs. (23) and (24). The arrows indicate the dipole-allowed transition from $|\text{GS}\rangle$ (black line) to $|\Phi^\pm_A\rangle$ [red (light gray) lines]. $|\Phi^\pm_a\rangle$ [blue (dark gray) lines] are dipole inactive. (b) FIR spectra for increasing magnetic field B. The anticrossing is clearly shown. A Lorentz profile function $\Gamma/\pi[(\omega-\omega_{fi})-\Gamma^2]$ is used to replace the δ function. The phenomenological broadening factor $\Gamma=0.2$ meV. Spectra are normalized to their maxima and offset for clarity.

$$\alpha(\omega) \propto \omega\sum_f |\langle f|H'|i\rangle|^2\delta(\omega-\omega_{fi}). \tag{28}$$

Here, $\hbar\omega_{fi} = E_f - E_i$, $|i\rangle = |\text{GS}\rangle$ is the ground state, and $|f\rangle$ stands for the excited states. We will focus on the four lowest excited states $|\Phi^\pm_A\rangle$ and $|\Phi^\pm_a\rangle$. According to Eqs. (7) and (8), the perturbation H' is obtained as

$$H' = \hbar\,\Omega\sqrt{\frac{\omega_0}{\Omega}}\left(1 - \frac{\omega_c}{\Omega}\right)A^+ + \alpha\sqrt{\frac{2m_0\omega_0}{\hbar}}(\sigma_{1+} + \sigma_{2+}). \tag{29}$$

Note that we have omitted the terms related to the B and b modes, which are not involved in the initial and final states we are considering, and thus do not contribute to the absorption coefficient. Our analytical results give the FIR spectra obvious physical meanings. From Eq. (29) above, we find that the first term is spin independent, and it provides a c.m. angular momentum excitation. This c.m. angular momentum excitation, which is the consequence of the Kohn theorem,[21] exists even in the absence of SOI. The second term, which is spin dependent, is due to the presence of SOI. This term contributes an excitation of the two spins *symmetrically*, i.e., $|\downarrow\downarrow\rangle \mapsto |\uparrow\downarrow\rangle + |\downarrow\uparrow\rangle$. Thus, H' only couples the ground state $|\text{GS}\rangle$ with the c.m. excited states $|\Phi^\pm_A\rangle$, while $|\Phi^\pm_a\rangle$ are inactive in this case. The matrix elements of $\langle\Phi^\pm_A|H'|\text{GS}\rangle$ are calculated, and the FIR spectra are shown in Fig. 3(b).

IV. QUANTUM ENTANGLEMENT IN LARGE-DETUNING LIMIT

Due to the linearly increase of the dimension of the invariance subspace $V^{(N)}$ with respect to N, it is difficult to obtain a compact solution of the eigenvalue problem for $N \geq 1$. Instead of the exact solution, the approximate solution by perturbation theory will be given in this section. In the region where perturbation treatment is valid, we derive an effective transverse spin-spin interaction Hamiltonian. This Hamiltonian can induce a two-qubit logic gate, and can be used to produce a controllable quantum entanglement.

We summarize the Hamiltonian obtained:

$$H_0 = H_{\text{orbit}} + \frac{1}{2}\hbar\,\omega_z(\sigma_{1z} + \sigma_{2z}), \tag{30}$$

$$H_1 = g_A A(\sigma_{1+} + \sigma_{2+}) + g_a a(\sigma_{1+} - \sigma_{2+}) + \text{H.c.}, \tag{31}$$

and then consider its reduction in the large-detuning limit, i.e., $\Delta_{A,a} \gg g_{A,a}$. In this limit, we perform the Fröhlich transformation with the operator

$$S = \left(\frac{g_A}{\Delta_A}A^\dagger(\sigma_{1-} + \sigma_{2-}) + \frac{g_a}{\Delta_a}a^\dagger(\sigma_{1-} - \sigma_{2-})\right) - \text{H.c.} \tag{32}$$

and the effective Hamiltonian $\exp(-S)H\exp(S)$ is calculated up to the second order as

$$H_S \simeq H_0 + \frac{1}{2}[H_1, S]. \tag{33}$$

Here, the second term in the right-hand side (RHS) can be written explicitly as

$$\begin{aligned}\frac{1}{2}[H_1,S] = {} & \hbar\,\xi(\sigma_{1+}\sigma_{2-} + \sigma_{1-}\sigma_{2+}) + \frac{g_A g_a}{2}\left(\frac{1}{\Delta_A} + \frac{1}{\Delta_a}\right)(A^\dagger a \\ & + a^\dagger A)(\sigma_{1z} - \sigma_{2z}) + \left(\frac{g_A^2}{\Delta_A}(A^\dagger A + 1/2) + \frac{g_a^2}{\Delta_a}(a^\dagger a \right. \\ & \left. + 1/2)\right)(\sigma_{1z} + \sigma_{2z}) + \left(\frac{g_A^2}{\Delta_A} + \frac{g_a^2}{\Delta_a}\right).\end{aligned} \tag{34}$$

Note that the first term of Eq. (34) is the effective transverse spin-spin coupling induced by SOI. The effective coupling strength

$$\hbar\,\xi = g_A^2/\Delta_A - g_a^2/\Delta_a \tag{35}$$

depends on (i) the SOI strength α [see Eqs. (13) and (14)], and (ii) the frequency difference between ω_A and ω_a, which is a consequence of the Coulomb interaction. We note that, in the subspace $V^{(0)}$, the second term of Eq. (34) vanishes, and the remaining terms commute with the total spin $\boldsymbol{\sigma}^2 = (\boldsymbol{\sigma}_1 + \boldsymbol{\sigma}_2)^2$. Thus we can denote the eigenstates by the spin singlet $|S\rangle = (|\uparrow\downarrow\rangle - |\downarrow\uparrow\rangle)/\sqrt{2}$ and triplet $|T_0\rangle = (|\uparrow\downarrow\rangle + |\downarrow\uparrow\rangle)/\sqrt{2}$, $|T_1\rangle = |\uparrow\uparrow\rangle$, and $|T_{-1}\rangle = |\downarrow\downarrow\rangle$ in the large-detuning limit in subspace $V^{(0)}$. Diagonalizing the Hamiltonian (34), we obtain the eigenenergies

$$E_{|T_{-1}^A\rangle} = -\Delta_A - \frac{2g_A^2}{\Delta_A}, \tag{36}$$

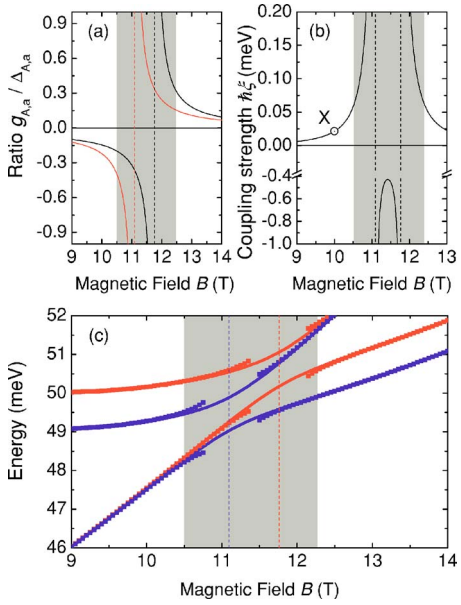

FIG. 4. (Color online) (a) The ratio g_A/Δ_A (black line) and g_a/Δ_a [red (gray) line]. The perturbation treatment is valid when both g_A/Δ_A and g_a/Δ_a are less than unity. (b) The effective transverse spin coupling strength induced by SOI. (c) A comparison of eigenenergies between exact [Eqs. (23) and (24), lines] and perturbative [Eqs. (36)–(39), scattered dots] solutions in the large-detuning region. Our perturbation treatment is valid in the unshaded region.

$$E_{|T_{-1}^a\rangle} = -\Delta_a - \frac{2g_a^2}{\Delta_a}, \tag{37}$$

$$E_{|T_0\rangle} = \frac{2g_A^2}{\Delta_A}, \tag{38}$$

$$E_{|S\rangle} = \frac{2g_a^2}{\Delta_a} \tag{39}$$

for the different spin states corresponding to the exact solutions in Eq. (24). Here, we also omit the zero-point energies.

The above energies are drawn as functions of magnetic field in Fig. 4(c) in comparison with the exact solutions. The exact consistency of the two solutions in the large-detuning region confirms the validity of our perturbation treatment. Figure 4(b) shows the effective spin coupling strength induced by SOI in our model. Taking $B = 10$ T for example [the point denoted by X in Fig. 4(b)], we have the spin coupling strength $\hbar\xi \simeq 20\ \mu$eV. This value is comparable with that in the proposal of the spin-spin coupling induced by electromagnetic field in cavity.[15] Thus, it is feasible to realize the two-qubit gate operation during the long coherence time of conduction band electrons.

The spin transverse coupling described by the first term in the RHS of Eq. (34) generates an ideal $\sqrt{i\text{SWAP}}$ gate[16,22] at a specific time $t_0 = \pi/4\xi$. On the other hand, it is worthy of notice that the unitary transformation $\exp(-S)H\exp(S)$ may induce an excitation of the boson modes, and then cause gate error during the time evolution of the spin states. To explic-

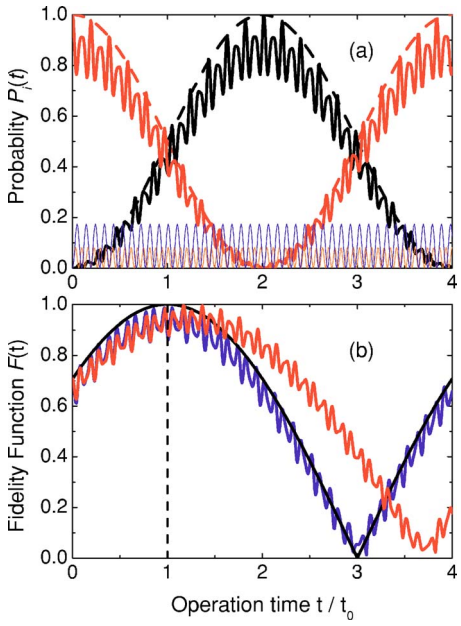

FIG. 5. (Color online) (a) Probability $P_i(t)$ as a function of t. Black, red solid lines represent the probabilities of $|0_A,0_a,\uparrow\downarrow\rangle$ and $|0_A,0_a,\downarrow\uparrow\rangle$, respectively. Blue and orange solid lines, which are below 0.2, represent the probabilities of $|1_A,0_a,\downarrow\downarrow\rangle$ and $|0_A,1_a,\downarrow\downarrow\rangle$, respectively. The dashed lines are the probabilities generated by the standard $\sqrt{i\text{SWAP}}$ gate. (b) Gate fidelity as a function of t. The black line indicates the ideal $\sqrt{i\text{SWAP}}$ operation. The blue and red lines represent the fidelity function generated by the second-order approximation Hamiltonian and the original Hamiltonian (see text), respectively.

itly show the unwanted boson mode excitations and to examine the reliability of our model, we consider the time evolution of the initial state $|\psi(0)\rangle=|0_A,0_a,\downarrow\uparrow\rangle$:

$$|\psi(t)\rangle = U(t)|\psi(0),$$

where

$$U(t) = \exp[-it(e^S H_S e^{-S})/\hbar] = e^S \exp(-itH_S/\hbar)e^{-S}. \tag{40}$$

Notice that $|\psi(0)\rangle$ belongs to the subspace $V^{(0)}$, and the time evolution will be restricted in this subspace. Figure 5(a) gives the probabilities $P_i(t)=|\langle i|\psi(t)\rangle|^2$ of finding state $|i\rangle$ at time t, where $|i\rangle$ stands for the four bases of the subspace $V^{(0)}$: $|0_A,0_a,\uparrow\downarrow\rangle$, $|0_A,0_a,\downarrow\uparrow\rangle$, $|1_A,0_a,\downarrow\downarrow\rangle$, and $|0_A,1_a,\downarrow\downarrow\rangle$, respectively. Besides the states $|0_A,0_a,\uparrow\downarrow\rangle$ and $|0_A,0_a,\downarrow\uparrow\rangle$, the unwanted boson mode excitation states $|1_A,0_a,\downarrow\downarrow\rangle$ and $|0_A,1_a,\downarrow\downarrow\rangle$ also have nonzero populations. These populations will induce the gate error. Furthermore, we calculate the fidelity function defined by

$$F(t) = |\langle\psi(0)|U^{+}_{\sqrt{i\text{SWAP}}}U(t)|\psi(0)\rangle|, \tag{41}$$

where $U_{\sqrt{i\text{SWAP}}}$ is the ideal $\sqrt{i\text{SWAP}}$ gate operator. We notice that the fidelity function $F(t)$ reaches its maximum at slightly less than unity at $t=t_0$, and the high-frequency oscillations appear due to the boson mode excitations mentioned above. We also examine the fidelity function generated by the original Hamiltonian (31), i.e., $U(t)=\exp[-it(H_0+H_1)/\hbar]$. In this case the original Hamiltonian (31) gives a high fidelity $F(t')\simeq 1$ at a different time $t'\simeq 1.2t_0$, which can be regarded as a higher-order correction in comparison to the approximate Hamiltonian (33). Finally, Fig. 5 shows that spin entanglement can be created in this system by adjusting the operation time.

V. CONCLUSION

In this paper, we have considered a system of two vertically CQDs each containing an electron in the presence of Rashba-type SOI. We have theoretically demonstrated that it is possible to create spin entanglement in this kind of system by using the SOI. In the large-interdot-separation case, the Coulomb interaction between the two electrons is approximately expressed in a quadratic form. Then the two-boson–two-spin interacting model is derived in the RWA from the original Hamiltonian. We give the exact solutions of the low excited states analytically. These solutions help us reveal the physics underlying the FIR spectra near the resonant point. A perturbation treatment in the large-detuning case shows that, as for a quantum dot embedded in an optical cavity, the orbital degrees of freedom play the role of a quantized data bus via the Coulomb interaction and the SOI in this system. The effective Hamiltonian of the spin-spin interaction is obtained by eliminating the orbital degrees of freedom. This Hamiltonian provides a two-qubit operation, which is essential in quantum information processing.

Finally, we would like to point out that using the effective interspin coupling to create spin entanglement is feasible to be controlled and measured. From the discussions above, we know that the effective spin coupling strength can be controlled by external magnetic field. On the other hand, the tunable strength α of the SOI,[3] in principle, also enables us to switch on and off the effective interspin coupling by external gates conveniently. To probe the quantum entanglement of spin systems, a similar method to the protocol proposed in Ref. 23 can be used, where the information stored in the spin degrees of freedom is converted to the charge states, and then the charge states can be detected.

ACKNOWLEDGMENTS

This work is funded by NSFC with Grants No. 90203018, No. 10474104, No. 60433050, No. 10374057, and No. 10574077, and NFRPC with Grants No. 2001CB309310, No. 2005CB724508, and No. 2005CB623606.

[1] I. Zutic, J. Fabian, and S. Das Sarma, Rev. Mod. Phys. **76**, 323 (2004).
[2] D. D. Awschalom, N. Samarth, and D. Loss, *Semiconductor Spintronics and Quantum Computation* (Springer-Verlag, Berlin, 2002).
[3] S. Debald and C. Emary, Phys. Rev. Lett. **94**, 226803 (2005).
[4] M. Governale, Phys. Rev. Lett. **89**, 206802 (2002).
[5] P. Lucignano, B. Jouault, A. Tagliacozzo, and B. L. Altshuler, Phys. Rev. B **71**, 121310(R) (2005).
[6] T. Chakraborty and Pekka Pietilainen, Phys. Rev. Lett. **95**, 136603 (2005).
[7] P. Pietilanen and T. Chakraborty, cond-mat/0509170 (unpublished).
[8] T. Chakraborty and P. Pietilainen, Phys. Rev. B **71**, 113305 (2005).
[9] P. Stano and J. Fabian, Phys. Rev. B **72**, 155410 (2005).
[10] J. Splettstoesser, M. Governale, and U. Zülicke, Phys. Rev. B **68**, 165341 (2003).
[11] S. Debald and B. Kramer, Phys. Rev. B **71**, 115322 (2005).
[12] M. Bayer, P. Hawrylak, K. Hinzer, S. Fafard, M. Korkusinski, Z. R. Wasilewski, O. Stern, and A. Forchel, Science **291**, 451 (2001); J.-L. Zhu, W. Chu, Z. Dai, and D. Xu, Phys. Rev. B **72**, 165346 (2005); X. Li, Y. Wu, D. Steel, D. Gammon, T. H. Stievater, D. S. Katzer, D. Park, C. Piermarocchi, and L. J. Sham, Science **301**, 809 (2003).
[13] W. Yao, R. Liu, and L. J. Sham, Phys. Rev. Lett. **92**, 217402 (2004); W. Yao, R. B. Liu, and L. J. Sham, *ibid.* **95**, 030504 (2005); R.-B. Liu, W. Yao, and L. J. Sham, Phys. Rev. B **72**, 081306(R) (2005).
[14] Y. Li, T. Shi, B. Chen, Z. Song, and C.-P. Sun, Phys. Rev. A **71**, 022301 (2005); T. Shi, Y. Li, Z. Song, and C.-P. Sun, *ibid.* **71**, 032309 (2005); Z. Song, P. Zhang, T. Shi, and C.-P. Sun, Phys. Rev. B **71**, 205314 (2005).
[15] A. Imamoglu, D. D. Awschalom, G. Burkard, D. P. DiVincenzo, D. Loss, M. Sherwin, and A. Small, Phys. Rev. Lett. **83**, 4204 (1999).
[16] O. Gywat, F. Meier, D. Loss, and D. D. Awschalom, Phys. Rev. B **73**, 125336 (2006); G. Burkard and Atac Imamoglu, cond-mat/0603119 (unpublished).
[17] N. F. Johnson and M. C. Payne, Phys. Rev. Lett. **67**, 1157 (1990).
[18] B. L. Johnson and G. Kirczenow, Phys. Rev. B **47**, 10563 (1993).
[19] L. Wendler, V. M. Fomin, A. V. Chaplik, and A. O. Govorov, Phys. Rev. B **54**, 4794 (1996).
[20] H. Hu, J.-L. Zhu, and J.-J. Xiong, Phys. Rev. B **62**, 16777 (2000).
[21] L. Jacak, P. Hawrylak, and A. Wojs, *Quantum Dots* (Springer-Verlag, Berlin, 1998).
[22] A. Blais, R.-S. Huang, A. Wallraff, S. M. Girvin, and R. J. Schoelkopf, Phys. Rev. A **69**, 062320 (2004).
[23] H-A. Engel and D. Loss, Science **309**, 586 (2005).